$10BaF_2$:NaF, Na_3AlF_6/TiO_2 composite as a novel visible-light-driven photocatalyst based on upconversion emission*

Liu En-Zhou(刘恩周)[a], Fan Jun(樊 君)[a]†, Hu Xiao-Yun(胡晓云)[b], Hou Wen-Qian(侯文倩)[a], and Dai Hong-Zhe(代宏哲)[a]

[a] *School of Chemical Engineering, Northwest University, Xi'an* 710069, *China*
[b] *Department of Physics, Northwest University, Xi'an* 710069, *China*

(Received 31 July 2011; revised manuscript received 23 November 2011)

A rare-earth free upconversion luminescent material, $10BaF_2$:NaF, Na_3AlF_6, is synthesized by a hydrothermal method. The study of fluorescent spectrum indicates that it can convert visible light (550 nm–610 nm) into ultraviolet light (290 nm–350 nm), and two emission peaks at 304 nm and 324 nm are observed under the excitation of 583 nm at room temperature. Subsequently, $10BaF_2$:NaF, Na_3AlF_6/TiO_2 composite photocatalyst is prepared and its catalytic activity is evaluated by the photocatalytic reduction of CO_2 under visible light irradiation ($\lambda > 515$ nm). The results show that $10BaF_2$:NaF, Na_3AlF_6/TiO_2 is a more effective photocatalyst for CO_2 reduction than pure TiO_2, their corresponding methanol yields are 179 and 0 μmol/g-cat under the same conditions. Additionally, the mechanism of photocatalytic reduction of CO_2 on $10BaF_2$:NaF, Na_3AlF_6/TiO_2 is proposed.

Keywords: rare-earth free upconversion luminescent material, ultraviolet emission, titanium dioxide, photocatalytic reduction of CO_2

PACS: 34.50.Lf, 42.70.–a, 89.20.–a **DOI:** 10.1088/1674-1056/21/4/043403

1. Introduction

Since photoinduced decomposition of water on TiO_2 electrode was discovered,[1] semiconductor-based photocatalysis has attracted great attention over the past few decades. Most of the investigations have focused on TiO_2 due to its relatively high reactivity, physical and chemical stability, low toxicity and cheapness.[2,3] However, TiO_2 has a relatively large band gap (3.2 eV) that requires ultraviolet (UV) light ($\lambda < 387$ nm) for activation, and the percentage of UV light in the solar spectrum is only 5%, which is very low compared with that of the visible light (∼48%). The low-usage of sunlight has been restraining the photocatalytic efficiency of pure TiO_2.[4] Therefore, many efforts have been made to develop the TiO_2 for the utilization of visible light, such as doping of metal or nonmetal elements,[5] surface photosensitization,[6] and combination with narrow band gap semiconductors.[7] This work does succeed in broadening the range of absorption wavelength of TiO_2. Unfortunately, the photopotential energy excited by visible light is lower than that by UV light according to the formula $E_g = h\nu$, where h is Planck constant and ν the light frequency, thus the reactivity of electron–hole pairs excited by visible light is relatively poor.[8,9]

Recently, much attention has been paid to extending the photo-response range of TiO_2 by upconversion luminescent material (ULM).[8−17] The upconversion luminescent materials $Y_3Al_5O_{12}$:Er^{3+}, Y_2O_3:Er^{3+}, $YAlO_3$:Er^{3+}, $NaYF_4$:Er^{3+}, and $40CdF_2 \cdot 60BaF_2 \cdot xEr_2O_3$ (x = 0.8, 1.0, and 1.2) have been employed to modify the TiO_2 photocatalyst; these upconversion luminescent materials could convert visible light into UV light and activate TiO_2 to generate electron–hole pairs, and the composite of ULM and TiO_2 exhibit higher activity than pure TiO_2 in degradation of organic days under the visible light irradiation. Nevertheless, the research has focused on the ULM with rare-earth elements for their abundant energy levels in the infrared-UV range.[18−23]

*Project supported by the National Natural Science Foundation of China (Grant No. 20876125), the Research Fund for the Doctoral Program of Higher Education, China (Grant No. 20096101110013), and the Northwest University Graduate Interdisciplinary Funds, China (Grant Nos. 09YJC24 and 09YJC27).

†Corresponding author. E-mail: fanjun@nwu.edu.cn

© 2012 Chinese Physical Society and IOP Publishing Ltd

In the present paper, a rare-earth free ULM (BaF_2:$Na_xAl_yF_{x+3y}$, $0.3 < x < 0.5$, $0 < y < 0.1$) is prepared and its fluorescence property is investigated. Subsequently, a visible-light-driven composite photocatalyst (BaF_2:$Na_xAl_yF_{x+3y}$/TiO_2) is prepared and its photocatalytic activity is tested as well; the photocatalytic reduction of CO_2 under visible light irradiation is found to be effective.

2. Experiment

2.1. Chemicals

All the chemicals were used as original ones without further purification. NaOH, Al_2O_3, BaF_2, and HF (40%) were all purchased from Sinopharm Chemical Reagent Co., Ltd (Shanghai, China).

2.2. Preparation of upconversion luminescent material BaF_2:$Na_xAl_yF_{x+3y}$

The upconversion luminescent material BaF_2:$Na_xAl_yF_{x+3y}$ was synthesized by a hydrothermal method. A mixture of NaOH (12.0 g) and Al_2O_3 (2.0 g) was added into 50 mL of distilled water, then stirred vigorously and refluxed at 200 °C for 6 h. BaF_2 (2.0 g) was dispersed into the above solution and kept stirring for 1 h. Subsequently, HF was used to adjust the pH to 1–2. After stirring for 2 h, the mixture was sealed in a 100-mL Teflon-lined stainless steel vessel, which can resist pressure. It was heated at 180 °C under a high pressure for 24 h and then cooled down to room temperature in a natural manner. The resulting precipitate was separated by centrifugation, washed with distilled water twice, and dried at 50 °C for 24 h in a vacuum oven with a pressure of 0.08 MPa. Finally, BaF_2:$Na_xAl_yF_{x+3y}$ was obtained by annealing the particles at 500 °C for 3 h, where x and y denote the atom percentages of Na and Al in $Na_xAl_yF_{x+3y}$ respectively.

2.3. Preparation of composite photocatalyst BaF_2:$Na_xAl_yF_{x+3y}$/TiO_2

Nano-TiO_2 (0.4 g, Degussa P25) and BaF_2:$Na_xAl_yF_{x+3y}$ (2.0 g) were mixed in 50-mL absolute alcohol, and adequately dispersed by ultrasound at a 40-kHz frequency and 300-W output power for 10 min, followed by centrifugation at 6000 rpm for 5 min, then the separated powder was dried at 50 °C for 12 h in a vacuum oven with a pressure of 0.08 MPa. BaF_2:$Na_xAl_yF_{x+3y}$/TiO_2 was obtained by annealing the particles at 400 °C for 3 h. For comparison, BaF_2:$Na_xAl_yF_{x+3y}$ and TiO_2 were treated under the same condition as described above.

2.4. Visible light photocatalytic activity

The visible light photocatalytic activities of the samples, including pure nano TiO_2, BaF_2:$Na_xAl_yF_{x+3y}$, and BaF_2:$Na_xAl_yF_{x+3y}$/TiO_2, were evaluated by photocatalytic reduction of CO_2 with H_2O in a circulated quartz photoreactor. The reactor was illuminated by a 500-W spherical xenon lamp with an optical filter $\lambda > 515$ nm, and shielded by a black box during the reaction to prevent the reactor from being interfered with by outside light. The 2.0 g of the photocatalyst was suspended in 400 mL of distilled water. Prior to irradiation, CO_2 (99.995%) was bubbled through the reactor for at least 30 min to eliminate dissolved oxygen and saturate the solution. The temperature was monitored and controlled by a temperature controller. During the experiment, some reaction solution evaporated into a condensed solution, which was analysed using gas chromatography directly.

2.5. Characterization

The general morphologies of the samples were characterized by a field-emission scanning electron microscope (FESEM, FEI, Quanta 400 FEG). X-ray diffraction (XRD) patterns were recorded using a Bruker D8 Advance Diffractometer with high-intensity Cu $K_{\alpha 1}$ irradiation ($\lambda = 1.5406$ Å, 1 Å = 0.1 nm). Room temperature upconversion luminescence properties were observed using a Hitachi F-7000 fluorescence spectrophotometer. Infrared spectra (IR) were recorded on a Fourier transform (FT) infrared spectrophotometer using KBr pellets (Bruker, VERTEX 70). The methanol yield was analysed by a gas chromatography, a Shimadzu GC-14C with hydrogen flame and PEG 20M column. The temperatures of column, injector, and detector were 90, 150, and 180 °C, respectively.

3. Results and discussion

3.1. Microstructure analysis

The size and morphology of the resulting materials were examined by scanning electron microscopy

(SEM). It is apparent that BaF_2:$Na_xAl_yF_{x+3y}$ consists of a large number of micro-particles which tend to adhere to each other (Fig. 1(a)). However, their surfaces become rough after the treatment described in Subsection 2.2 (Fig. 1(b)). It is indicated that TiO_2 nano-particles may be coated on the surface of the BaF_2:$Na_xAl_yF_{x+3y}$ particle after the ultrasonic dispersion and annealing treatment. The coupling between TiO_2 and BaF_2:$Na_xAl_yF_{x+3y}$ is probably due to the formation of the chemical bonds (refer FT–IR analyses below).

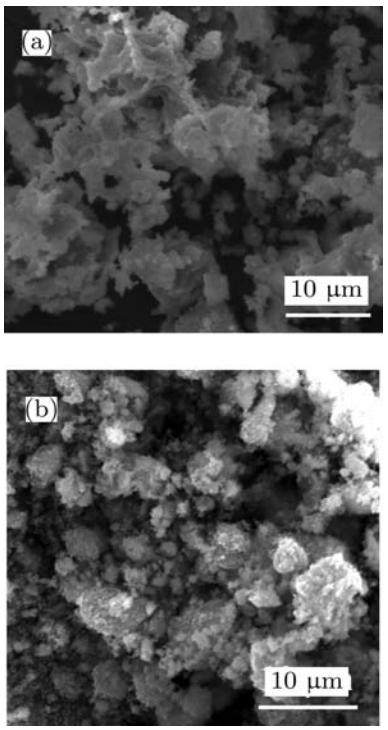


Fig. 1. SEM images of (a) BaF_2:$Na_xAl_yF_{x+3y}$ and (b) BaF_2:$Na_xAl_yF_{x+3y}$/TiO_2.

The FT–IR spectra of the samples are shown in Fig. 2. The absorption peak at 1630 cm^{-1} belongs to the bending vibration of the hydroxyl group on the surface of the samples. The peak centred at 663 cm^{-1} is due to vibration absorption of O–Ti–O bands.[24] The peaks at 413 cm^{-1} and 578 cm^{-1} are attributed to the bending and the stretching vibration absorptions of BaF_2 and $[AlF_6]^{3-}$, respectively. As shown in Fig. 2 (curve *c*), two small absorption peaks at 906 cm^{-1} and 946 cm^{-1} are observed in the spectrum of BaF_2:$Na_xAl_yF_{x+3y}$/TiO_2 compared with the spectra of TiO_2 and BaF_2:$Na_xAl_yF_{x+3y}$, which can be attributed to the stretching vibration absorptions of Al–O and F–O bands on the contact surface between TiO_2 and BaF_2:$Na_xAl_yF_{x+3y}$. It means that TiO_2 is attached to BaF_2:$Na_xAl_yF_{x+3y}$ under the assistance of chemical bonds, which might cause the shift of O–Ti–O infrared feature toward lower frequencies (643 cm^{-1}) in the spectrum of BaF_2:$Na_xAl_yF_{x+3y}$/TiO_2. The peak at 1096 cm^{-1} is basically retained. These results suggest that the main properties of TiO_2 and BaF_2:$Na_xAl_yF_{x+3y}$ are not changed in the composite photocatalyst.

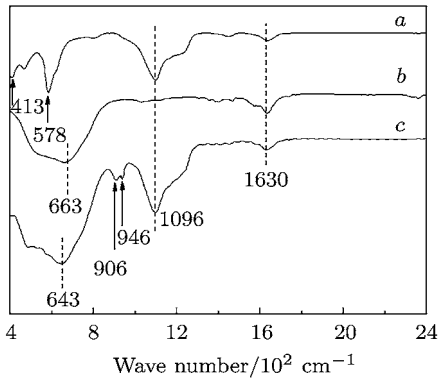


Fig. 2. FT–IR spectra of (curve *a*) BaF_2:$Na_xAl_yF_{x+3y}$, (curve *b*) Nano-TiO_2, and (curve *c*) BaF_2:$Na_xAl_yF_{x+3y}$/TiO_2.

The XRD patterns of the sample are shown in Fig. 3. The characteristic diffraction peaks of BaF_2, NaF, and Na_3AlF_6 are observed in the XRD pattern of BaF_2:$Na_xAl_yF_{x+3y}$ (Fig. 3(a)), which are in good agreement with those in the standard JCPDS cards Nos. 04–0452, 36–1455, and 25–0772, respectively. It is indicated that NaF and Na_3AlF_6 are obtained under the above conditions. Therefore, BaF_2:$Na_xAl_yF_{x+3y}$ is a ternary fluoride, including BaF_2, NaF, and Na_3AlF_6. Hereafter, $Na_xAl_yF_{x+3y}$ is employed to denote the NaF and Na_3AlF_6 for short. The XRD pattern of BaF_2:$Na_xAl_yF_{x+3y}$/TiO_2 is shown in Fig. 3(b). Clearly, in addition to the diffraction peaks of anatase TiO_2 (JCPDS No. 21–1272), and rutile TiO_2 (JCPDS No. 21–1276, 27.45°, 36.09°, and 54.32°), only several weak peaks of BaF_2 are observed at 24.86°, 28.78°, 41.13°, and 48.60°. Figure 4 shows the energy dispersive X-ray analysis (EDAX) pattern of the sample. The molar ratio of BaF_2, NaF, and Na_3AlF_6 is about 10:1:1 in BaF_2:$Na_xAl_yF_{x+3y}$ and the atom percentages of Na and Al in $Na_xAl_yF_{x+3y}$ are about 33.3% and 8.3%, respectively, and the formula of $Na_xAl_yF_{x+3y}$ is $Na_{0.333}Al_{0.083}F_{0.582}$ according to the atom percentage shown in the inset table of Fig. 4.

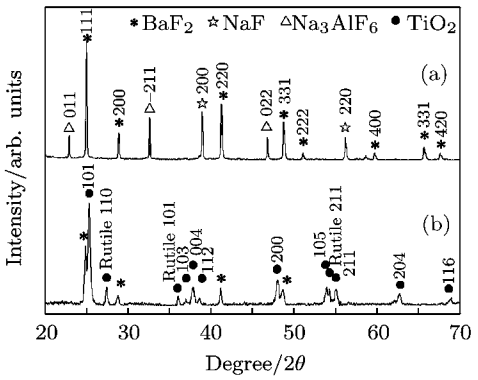


Fig. 3. XRD patterns of (a) BaF_2:$Na_xAl_yF_{x+3y}$ and (b) BaF_2:$Na_xAl_yF_{x+3y}$/TiO_2.

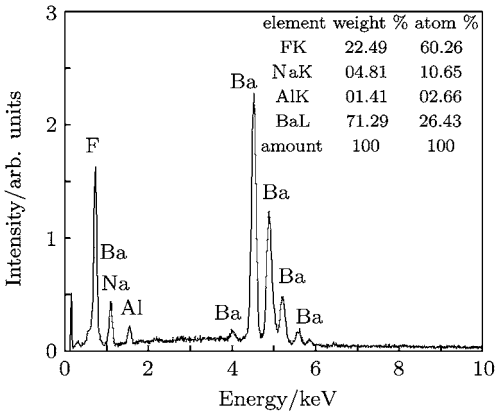


Fig. 4. EDAX pattern of BaF_2:$Na_xAl_yF_{x+3y}$.

3.2. Upconversion luminescence properties

Figure 5 shows the three-dimensional scan spectra of BaF_2:$Na_xAl_yF_{x+3y}$. The ordinate and the abscissa denote the excitation wavelength and the emission wavelength respectively. A continuous curve represents the same emission intensity. The emission ranges I and II in Fig. 5 are attributed to the Raman scattering. Besides, it can be seen clearly that the visible light (550 nm–610 nm) can be effectively converted into ultraviolet light (290 nm–350 nm) by BaF_2:$Na_xAl_yF_{x+3y}$. However, none of pure BaF_2, NaF, Na_3AlF_6, and their mixtures exhibit upconversion luminescence properties (See items (a1) to (a7) in Appendix A).

The excitation spectra of BaF_2:$Na_xAl_yF_{x+3y}$ were measured using the monitoring wavelength at 324 nm at different photomultiplier tube (PMT) voltages (See item (a8) in Appendix A). Two excitation peaks at 290 nm and 583 nm are found in the spectra, suggesting that there are two different energy levels in BaF_2:$Na_xAl_yF_{x+3y}$, which lead to the light absorptions at around 290 nm and 583 nm. The emission spectra and phosphorescence life time of BaF_2:$Na_xAl_yF_{x+3y}$ are presented in items (a9) and (a10) of Appendix A. It can be seen that the emission property under the excitation of 290 nm is very similar to that under the excitation of 583 nm, including the emission peaks and phosphorescence lifetime ($t > 3$ ms). These results suggest that the light emissions from BaF_2:$Na_xAl_yF_{x+3y}$ under the excitation of 290 nm and 583 nm undergo a similar emission process except for the excitation process (See item (a11) in Appendix A).

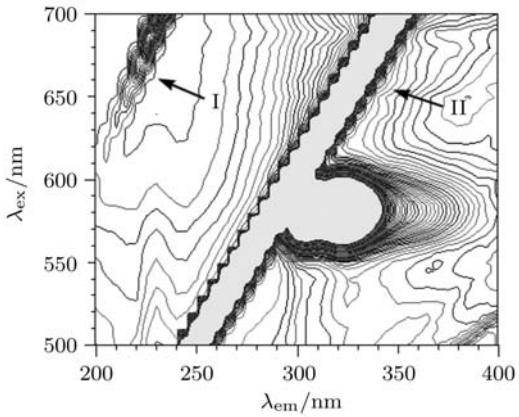


Fig. 5. Three-dimensional scan spectra of BaF_2:$Na_xAl_yF_{x+3y}$.

The energy levels of BaF_2:$Na_xAl_yF_{x+3y}$ in (item (a11)) of Appendix A may be related to the crystal defects of BaF_2 for its fluorite structure, which can be induced easily by the impurity ion (Na^+) and Frenkel disorder during the heat treatment. The light absorption at 583 nm is attributed to the F_A (Na^+) centre in the BaF_2 crystal,[25–27] and the light absorption at 290 nm and the radiative transition may result from other detectable levels.[28–31] It is likely that the electron in the excited state (ES_1) can absorb another 583 nm photon and transfer to ES_4, because the energy of ES_1 (2.13 eV) is about half that of ES_4 (4.28 eV). The transitions from ES_3 and ES_2 to the ground state (GS) result in the emissions at 304 nm and 324 nm. The above results suggest that the upconversion emissions may be related to the BaF_2 and Na^+. However, those detected levels in BaF_2 crystal are still elusive, further efforts on this perspective are needed.

The visible-light-driven photocatalysis based on upconversion emission depends on the energy transfer from BaF_2:$Na_xAl_yF_{x+3y}$ to TiO_2. The requirement for an efficient energy transfer is to make the

donor emission band overlap with the absorption band of the acceptor.[32,33] Here BaF_2:$Na_xAl_yF_{x+3y}$ is the donor and TiO_2 is the acceptor. The excitation spectrum and upconversion emission spectrum of BaF_2:$Na_xAl_yF_{x+3y}$, and the absorption spectrum of TiO_2 are presented in Fig. 6. As a semiconductor with a wide band gap, TiO_2 exhibits a narrow absorption band from 200 nm–400 nm (Fig. 6 (curve *a*)). It is very clear that the absorption band of TiO_2 overlaps very well with the UV emission of upconversion particles (Fig. 6 (curve *b*)), which can be excited by the visible light at around 583 nm (Fig. 6(curve *c*)). The large spectral overlap indicates that the upconversion UV emission can be strongly quenched by energy transfer.

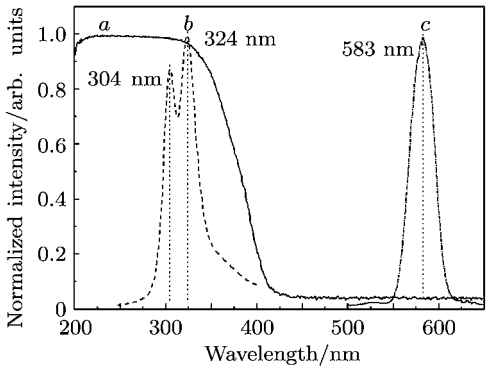


Fig. 6. (curve *a*) Absorption spectrum of TiO_2, (curve *b*) upconversion emission spectrum of BaF_2:$Na_xAl_yF_{x+3y}$, (curve *c*) excitation spectrum of BaF_2:$Na_xAl_yF_{x+3y}$.

To examine the energy transfer process, the upconversion emission spectra of the BaF_2:$Na_xAl_yF_{x+3y}$ and BaF_2:$Na_xAl_yF_{x+3y}$/TiO_2 were recorded under the excitation of 583 nm (Fig. 7). The intensities of

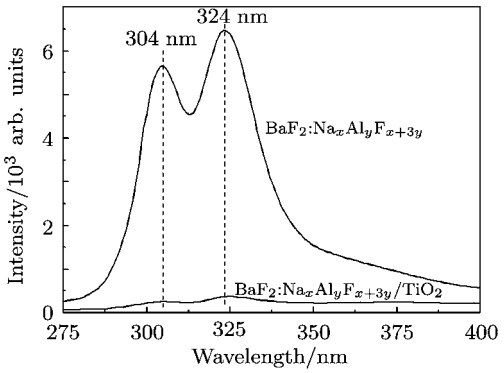


Fig. 7. The upconversion emission spectra of BaF_2:$Na_xAl_yF_{x+3y}$ and BaF_2:$Na_xAl_yF_{x+3y}$/TiO_2.

UV emission peaks are greatly reduced after the combination of TiO_2, indicating effective energy transfer from BaF_2:$Na_xAl_yF_{x+3y}$ to TiO_2. The comparison of the visible light photocatalytic activity between the donor and the donor–acceptor pairs could provide direct evidence for the energy transfer (refer Subsection 3.3).

3.3. Photocatalytic properties

The visible-light-driven photocatalytic activity of BaF_2:$Na_xAl_yF_{x+3y}$/TiO_2 composite was measured by the photocatalytic reduction of CO_2 with H_2O. GC analysis indicated that methanol was the major hydrocarbon. Figure 8 shows the methanol yield of the reaction under the visible light irradiation. It can be seen that BaF_2:$Na_xAl_yF_{x+3y}$/TiO_2 is obviously an effective photocatalyst for this reaction, the corresponding methanol yield increases fleetly at the beginning with the irradiation of visible light ($\lambda > 515$ nm), and reaches its maximum (179 μmol/g-cat) at 3.0 h. However, pure nano-TiO_2 and BaF_2:$Na_xAl_yF_{x+3y}$ do not show photocatalytic activity when used separately under the same conditions. It suggests that upconversion luminescence property is the main function mechanism of BaF_2:$Na_xAl_yF_{x+3y}$ during the photoreaction, which further confirms the energy transfer from BaF_2:$Na_xAl_yF_{x+3y}$ to TiO_2.

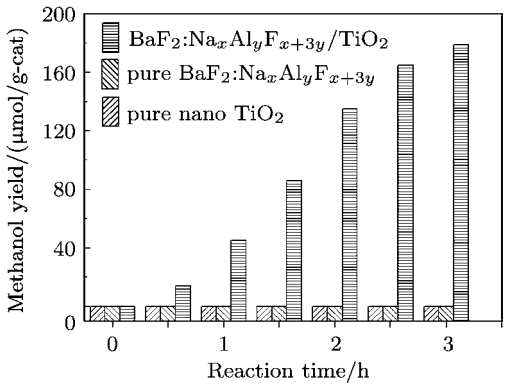


Fig. 8. Methanol yields of photocatalytic reaction of CO_2 with H_2O under the visible light irradiation ($\lambda > 515$ nm) at reaction temperature 40 °C, CO_2 flow rate about 10 mL/s. The methanol yield should be described as (methanol concentration)/(concentration of TiO_2).

3.4. Mechanism of photocatalytic reduction of CO_2 on BaF_2:$Na_xAl_yF_{x+3y}$/TiO_2

Firstly, the incident visible light (560 nm–610 nm) is converted into UV light (290 nm–350 nm) by BaF_2:$Na_xAl_yF_{x+3y}$ (Eq. (1)), then the UV light is absorbed by TiO_2 particles. Subsequently, electron (e^-)–hole (h^+) pairs are formed and located in the

conduction band and valence band of TiO_2 (Eq. (2)). Finally, redox reactions are initiated by e^- and h^+ on the surface of TiO_2. The active h^+ can oxidize H_2O or OH^- to form hydroxyl radicals ($OH\cdot$) which could release O_2 and H^+.[34] H^+ and high active e^- will facilitate CO_2 reduction and produce methanol or other hydrocarbons.[35–37] Equation (3) indicates that six electrons are required to convert the C^{4+} of CO_2 into the C^{2-} of CH_3OH. It is apparent that BaF_2:$Na_xAl_yF_{x+3y}$ plays a crucial role in the above process

$$4hv_{583\ \mathrm{nm}} \xrightarrow{BaF_2:Na_xAl_yF_{x+3y}} hv_{304\ \mathrm{nm}}+hv_{324\ \mathrm{nm}}, \quad (1)$$

$$TiO_2+hv_{304\ \mathrm{nm}}+hv_{324\ \mathrm{nm}} \rightarrow 2TiO_2(e^-)+2TiO_2(h^+), \quad (2)$$

$$CO_2 + 2H_2O + 6e^- \rightarrow CH_3OH + 3/2O_2. \quad (3)$$

4. Conclusions

The upconversion luminescent material 10BaF_2:NaF, Na_3AlF_6 is synthesized by a hydrothermal method, and 10BaF_2:NaF, Na_3AlF_6/TiO_2 composite is prepared for visible-light photocatalysis based on upconversion emission. The microstructure and the upconversion properties of the resulting samples are investigated. The energy transfer from 10BaF_2:NaF, Na_3AlF_6 to TiO_2 under visible light irradiation is confirmed. The visible-light-driven photocatalysis is realized by photocatalytic reduction of CO_2 with H_2O. This study suggests a promising method to develop the visible-light-driven photocatalysis, which may have a profound implication on the future utilization of solar energy.

Appendix A

(a1) Supporting information about the three-dimensional scan spectra of pure BaF_2 (Fig. (a1)).

(a2) Supporting information about the three-dimensional scan spectra of pure NaF (Fig. (a2)).

(a3) Supporting information about the three-dimensional scan spectra of pure Na_3AlF_6 (Fig. (a3)).

(a4) Supporting information about the three-dimensional scan spectra of the mixture of BaF_2 and NaF (10:1) (Fig. (a4)).

(a5) Supporting information about the three-dimensional scan spectra of the mixture of BaF_2 and Na_3AlF_6 (10:1) (Fig. (a5)).

(a6) Supporting information about the three-dimensional scan spectra of the mixture of NaF and Na_3AlF_6 (1:1) (Fig. (a6)).

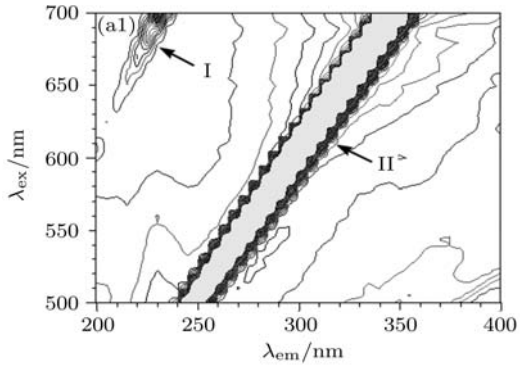
(a7) Supporting information about the three-dimensional scan spectra of the mixture of BaF_2, NaF, and Na_3AlF_6 (10:1:1) (Fig. (a7)).

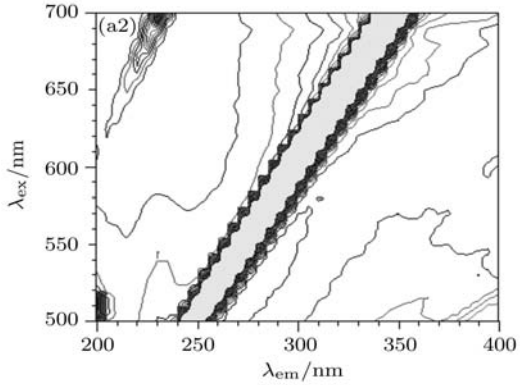
(a8) Supporting information about the excitation spectra of BaF_2:$Na_xAl_yF_{x+3y}$ (the monitoring wavelength is 324 nm) (Fig. (a8)).

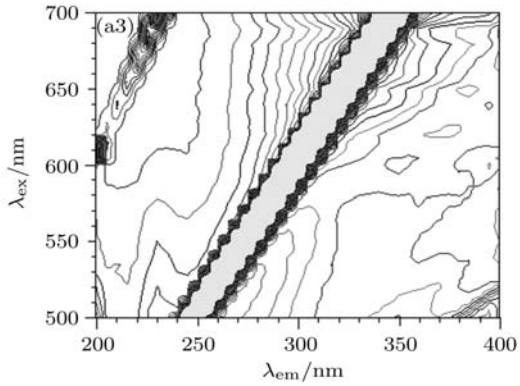
(a9) Supporting information about the emission spectrum of BaF_2:$Na_xAl_yF_{x+3y}$ (Fig. (a9)).

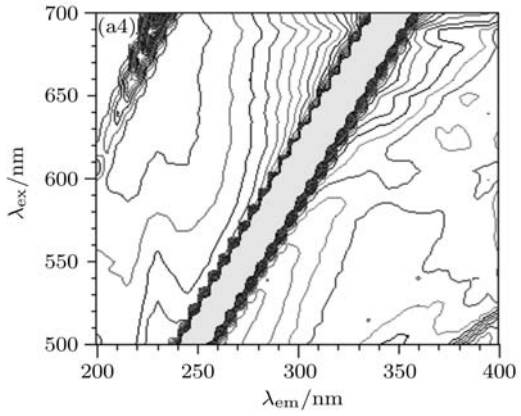
(a10) Supporting information about the phosphorescence life time of BaF_2:$Na_xAl_yF_{x+3y}$ (Fig. (a10)).

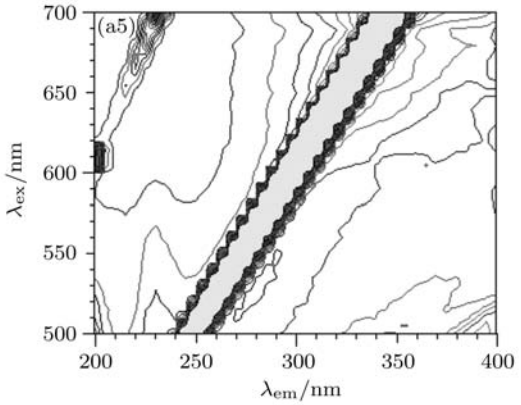
(a11) Supporting information about the emission process of BaF_2:$Na_xAl_yF_{x+3y}$ (Fig. (a11)).

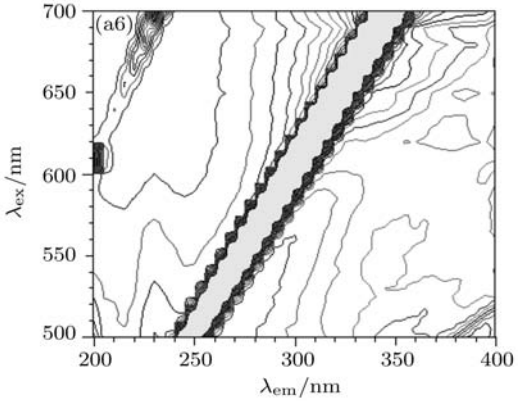


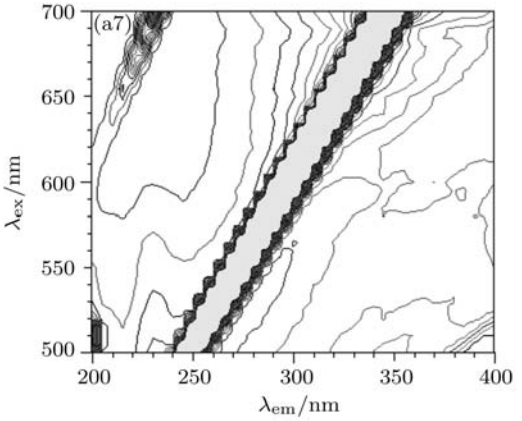


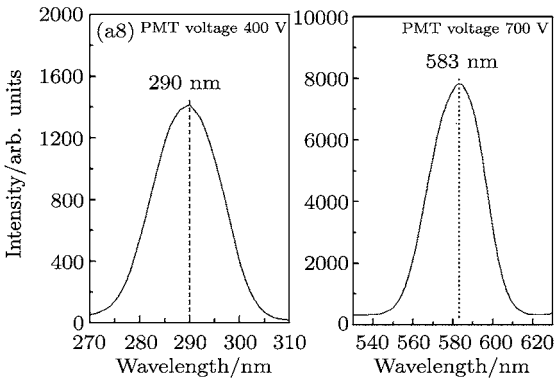


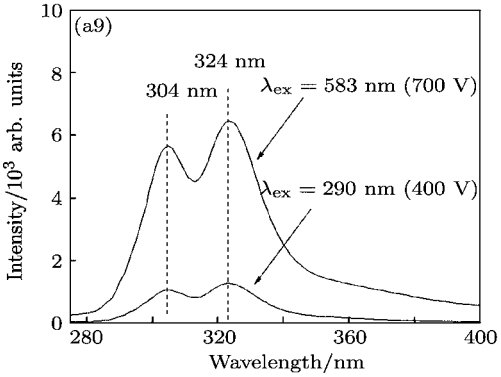


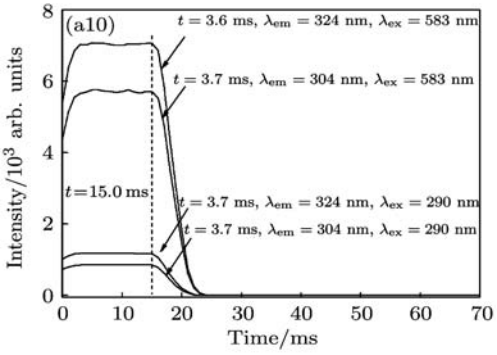












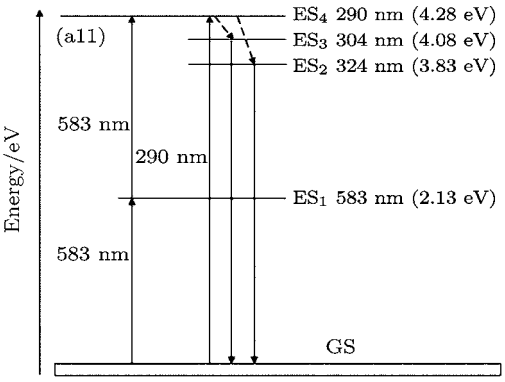


Fig. A1. The scan spectra for pure BaF_2, NaF, Na_3AlF_6, and their mixtures (a1)–(a7); the excitation spectra of BaF_2:$Na_xAl_yF_{x+3y}$ (a8); the emission spectra and phosphorescence life time of BaF_2:$Na_xAl_yF_{x+3y}$ (a9) and (a10); the energy levels of BaF_2:$Na_xAl_yF_{x+3y}$ (a11).

References

[1] Fujishima A and Honda K 1972 *Nature* **238** 37

[2] Linsebigler A L, Lu G and Yates J T 1995 *Chem. Rev.* **95** 735

[3] Wang J, Ma T, Zhang G, Zhang Z H, Zhang X D, Jiang Y F, Zhao G and Zhang P 2007 *Catal. Commun.* **8** 607

[4] Qin W P, Zhang D S, Zhao D, Wang L L and Zheng K Z 2010 *Chem. Commun.* **46** 2304

[5] Fan J, Liu E Z, Tian L, Hu X Y, He Q and Sun T 2010 *J. Environ. Eng-ASCE* **137** 171

[6] Nguyen T V, Wu J C S and Chiou C H 2008 *Catal. Commun.* **9** 2073

[7] Li G S, Zhang D Q and Yu J C 2009 *Environ. Sci. Technol.* **43** 7079

[8] Feng G J, Liu S W, Xiu Z L, Zhang Y, Yu J X, Chen Y G, Wang P and Yu X J 2008 *J. Phys. Chem.* C **112** 13692

[9] Wang J, Li R H, Zhang Z H, Sun W, Xu R, Xie Y P, Xing Z Q and Zhang X D 2008 *Appl. Catal.* A **334** 227

[10] Ye Y X, Liu E Z, Hu X Y, Yan Z Y, Jiang Z Y and Fan J 2011 *Chin. Sci. Bull.* **56** 1

[11] Wang J, Li J, Xie Y P, Li C W, Han G X, Zhang L Q, Xu R and Zhang X D 2010 *J. Environ. Manage.* **91** 677

[12] Xu R, Li J, Wang J, Wang X F, Liu B, Wang B X, Luan X Y and Zhang X D 2010 *Sol. Energy Mat. Sol.* C **94** 1157

[13] Qin W P, Zhang D S, Zhao D, Wang L L and Zheng K Z 2010 *Chem. Commun.* **46** 2304

[14] Wang J, Wen F Y, Zhang Z H, Zhang X D, Pan Z J, Zhang L, Wang L, Xu L, Kang P L and Zhang P 2005 *J. Environ. Sci.* **17** 727

[15] Wang J, Wen F Y, Zhang Z H, Zhang X D, Pan Z J, Zhang P, Kang P L, Tong J, Wang L and Xu L 2006 *J. Photochem. Photobiol.* A **180** 189

[16] Wang J, Zhang C H, Zhang G, Zhang X D, Zhao G, Ma T, Jiang Y F and Zhang P 2006 *Technol. Water Treat.* **32** 5 (in Chinese)

[17] Ye Y X, Hu X Y, Yan Z Y, Liu E Z, Fan J, Zhang D K, Miao H, Shang Y B and Yang J 2011 *Chin. Phys.* B **20** 087803

[18] Liu Q, Zhao L C, Guo F Y and Li M C 2009 *Chin. Phys.* B **18** 4030

[19] Liu L S, Lü S C and Sun J T 2010 *Acta Phys. Sin.* **59** 6637 (in Chinese)

[20] Auzel F 2003 *Chem. Rev.* **104** 139

[21] Zhou Y X, Dai S X, Zhou L, Xu T F, Nie Q H and Huang S L 2009 *Acta Phys. Sin.* **58** 1261 (in Chinese)

[22] Bünzli J C G and Eliseeva S V 2010 *J. Rare Earth* **28** 824

[23] Li T G, Liu S W, Wang E H and Song L J 2011 *Acta Phys. Sin.* **60** 073201 (in Chinese)

[24] Hu S Z, Wang A J, Li X and Löwe H 2010 *J. Phys. Chem. Solids* **71** 156

[25] Chen J, Lin L B and Jing F Q 2002 *Nucl. Instrum. Method* B **187** 354

[26] Zhang J, Lin L B, Jiang S J, Chen J, Liu M and Lin L Z 1998 *J. Syn. Crystals* **27** 330 (in Chinese)

[27] Chen J, Lin L B, Zhang J, He W and Lu Y 1999 *J. Syn. Crystals* **28** 233 (in Chinese)

[28] Arkhangelskaya V A and Feofilov P P 1980 *Sov. J. Quantum Electron.* **10** 657

[29] Arkhangelskaya V A, Fedorov A A and Feofilov P P 1979 *Opt. Commun.* **28** 87

[30] Ma Y and Rohlfing M 2008 *Phys. Rev.* B **77** 115118

[31] Vail J M, Coish W A, He H and Yang A 2002 *Phys. Rev.* B **66** 014109

[32] Kameta N, Masuda M, Minamikawa H, Mishima Y, Yamashita I and Shimizu T 2007 *Chem. Mater.* **19** 3553

[33] Oar M A, Serin J M, Dichtel W R, Fréchet J M J, Ohulchanskyy T Y and Prasad P N 2005 *Chem. Mater.* **17** 2267

[34] Wu J C S 2009 *Catal. Surv. Asia* **13** 30

[35] Anpo M, Yamashita H, Ichihashi Y and Ehara S 1995 *J. Electroanal. Chem.* **396** 21

[36] Tan S S, Zou L and Hu E 2006 *Catal. Today* **115** 269

[37] Zhang Q H, Han W D, Hong Y J and Yu J G 2009 *Catal. Today* **148** 335